Retrieving quasi-phase-matching structure with discrete layer-peeling method

Q. W. Zhang,[1] X. L. Zeng,[1,2,*] M. Wang,[1] T. Y. Wang,[1] and X. F. Chen[3]

[1]*The Key Lab of Specialty Fiber Optics and Optical Access Network, Shanghai University, Shanghai 200072, China*

[2]*DTU Fotonik, Department of Photonics Engineering, Technical University of Denmark, Lyngby 2800, Denmark*

[3]*Department of Physics, the State Key Laboratory on Fiber Optic Local Area Communication Networks and Advanced Optical Communication Systems, Shanghai Jiao Tong University, Shanghai 200240, China*

**zenglong@shu.edu.cn*

Abstract: An approach to reconstruct a quasi-phase-matching grating by using a discrete layer-peeling algorithm is presented. Experimentally measured output spectra of Šolc-type filters, based on uniform and chirped QPM structures, are used in the discrete layer-peeling algorithm. The reconstructed QPM structures are in agreement with the exact structures used in the experiment and the method is verified to be accurate and efficient in quality inspection on quasi-phase-matching grating.

OCIS codes: (230.2090) Electro-optical devices; (190.4360) Nonlinear optics, devices; (120.2440) Filters.

References and links

1. K. Mizuuchi, K. Yamamoto, M. Kato, and H. Sato, "Broadening of the Phase-Matching Bandwidth in Quasi-Phase-Matched Second-Harmoic Generation," IEEE J. Quantum Electron. **30**, 1596–1604 (1994).
2. S. N. Zhu, Y. Y. Zhu, and N. B. Ming, "Quasi-phase-matched third-harmonic generation in a quasi-periodic optical superlattice," Science **278**, 843–846 (1997).
3. M. Charbonneau-Lefort, M. M. Fejer, and B. Afeyan,"Tandem chirped quasi-phase-matching grating optical parametric amplifier design for simultaneous group delay and gain control," Opt. Lett. **30**, 634–636 (2005).
4. J. Huang, X. P. Xie, C. Langrock, R. V. Roussev, D. S. Hum, and M. M. Fejer, "Amplitude modulation and apodization of quasiphase-matched interactions," Opt. Lett. **31**, 604–606 (2006).
5. T. Umeki, M. Asobe, T. Yanagawa, O. Tadanaga, Y. Nishida, K. Magari, and H. Suzuki, "Broadband wavelength conversion based on apodized $\chi^{(2)}$ grating," J. Opt. Soc. Am. B **26**, 2315–2322 (2009).
6. X. Zeng, S. Ashihara, Z. Wang, T. Wang, Y. Chen, and M. Cha, "Excitation of two-colored temporal solitons in a segmented quasi-phase-matching structure, " Opt. Express **17**, 16877–16884 (2009).
7. Y. W. Lee, F. C. Fan, Y. C. Huang, B. Y. Gu, B. Z. Dong, and M. H. Chou, "Nonlinear multiwavelength conversion based on an aperiodic optical superlattice in lithium niobate," Opt. Lett. **27**, 2191–2193 (2002).
8. X. Zeng, X. Chen, F. Wu, Y. Chen, Y. Xia, and Y. Chen, "Second-harmonic generation with broadened flattop bandwidth in aperiodic domain-inverted gratings," Opt. Commun. **204**, 407–411 (2002).
9. A. M. Schober, G. Imeshev, and M. M. Fejer, "Tunable-chirp pulse compression in quasi-phase-matched second-harmonic generation," Opt. Lett. **27**, 1129–1131 (2002).
10. K. Beckwitt, F. Ö. Ilday, and F. W. Wise, "Frequency shifting with local nonlinearity management in nonuniformly poled quadratic nonlinear materials," Opt. Lett. **29**, 763–765 (2004).
11. X. Zeng, S. Ashihara, X. Chen, T. Shimura, and K. Kuroda, "Two-color pulse compression in aperiodically poled lithium niobate," Opt. Commun. **281**, 4499–4503 (2008).
12. H. Miao, S. Yang, C. Langrock, R. V. Roussev, M. M. Fejer, and A. M. Weiner, "Ultralow-power second-harmonic generation frequency-resolved optical gating using aperiodically poled lithium niobate waveguides," J. Opt. Soc. Am. B **25**, A41–A53 (2008).

#167192 - $15.00 USD Received 23 Apr 2012; revised 19 Jun 2012; accepted 21 Jun 2012; published 27 Jun 2012

13. J. Shaar, L. G. Wang, and T. Erdogan, "On the synthesis of fiber bragg gratings by layer peeling," IEEE J. Quantum Electron. **37**, 165–173 (2001).
14. J. Zhang, P. Shum, S. Y. Li, N. Q. Ngo, X. P. Cheng, and J. H. Ng, "Design and fabrication of flat-band long-period grating," IEEE Photon. Technol. Lett. **15**, 1558–1560 (2003).
15. H. Li, T. Kumagai, and K. Ogusu, "Advanced design of a multichannel fiber Bragg grating based on a layer-peeling method," J. Opt. Soc. Am. B **21**, 1929–1938 (2004).
16. Y. Choi, J. Chun, and J. Bae, "Numerically extrapolated discrete layer-peeling algorithm for synthesis of nonuniform fiber Bragg gratings," Opt. Express **19**, 8254–8266 (2011).
17. E. C. Levy and M. Horowitz, "Layer-peeling algorithm for reconstructing the birefringence in optical emulators," J. Opt. Soc. Am. B **23**, 1531–1539 (2006).
18. X. Chen, J. Shi, Y. Chen, Y. Zhu, Y. Xia, and Y. Chen, "Electro-optic Šolc-type wavelength filter in periodically poled lithium niobate," Opt. Lett. **28**, 2115–2117 (2003).
19. Y. Q. Lu and Z. L. Wan, "Electro-optic effect of periodically poled optical superlattice $LiNbO_3$ and its applications," Appl. Phys. Lett. **77**, 3719–3721 (2000).
20. Q. Zhang, X. Zeng, F. Pang, X. Chen, and T. Wang, "Tunable polarization-independent Šolc-type wavelength filter based on periodically poled lithium niobate," Opt. Laser Technol. **44**, 1992–1994 (2012).
21. C. H. Lin, Y. H. Chen, S. W. Lin, C. L. Chang, Y. C. Huang, and J. Y. Chang, "Electro-optic narrowband multi-wavelength filter in aperiodically poled lithium niobate," Opt. Express **15**, 9859–9866 (2007).
22. X. Gu, X. Chen, Y. Chen, X. Zeng, Y. Xia, and Y. Chen, "Narrowband multiple wavelengths filter in aperiodic optical superlattice," Opt. Commun. **237**, 53–58 (2004).
23. C. L. Chang, Y. H. Chen, C. H. Lin, and J. Y. Chang, "Monolithically integrated multi-wavelength filter and second harmonic generator in aperiodically poled lithium niobate," Opt. Express **16**, 18535–18544 (2008).
24. Y. L. Lee, Y. C. Noh, C. S. Kee, N. E. Yu, W. Shin, C. Jung, D. K. Ko, and J. Lee, "Bandwidth control of a Ti:PPLN Šolc filter by a temperature-gradient-control technique," Opt. Express **16**, 13699–13706 (2008).
25. C. Y. Huang, C. H. Lin, Y. H. Chen, and Y. C. Huang, "Electro-optic Ti:PPLN waveguide as efficient optical wavelength filter and polarization mode converter," Opt. Express **15**, 2548–2554 (2007).
26. C. S. Kee, Y. L. Lee, and J. Lee, "Electro- and thermo-optic effects on multi-wavelength Šolc filters based on $\chi^{(2)}$ nonlinear quasi-periodic photonic crystals," Opt. Express **16**, 6098–6103 (2008).
27. J. K. Brenne and J. Skaar, "Design of grating-assisted codirectional couplers with discrete inverse-scattering algorithms," J. Lightwave. Technol. **21**, 254–263 (2003).
28. G. Lenz, B. J. Eggleton, and C. R. Giles, "Dispersive properties of optical filters for WDM systems," IEEE J. Quantum Electron. **34**, 1390–1402 (1998).
29. L. Wang and T. Erdogan, "Layer peeling algorithm for reconstruction of long-period fibre gratings," Electron. Lett. **37**, 154–156 (2001).
30. T. Erdogan, "Fiber grating spectra," J. Lightwave Technol. **15**, 1277–1294 (1997).
31. R. Feced and M. N. Zervas, "Efficient inverse scattering algorithm for the design of grating-assisted co-directional mode couplers," J. Opt. Soc. Am. A **17**, 1573–1582 (2000).
32. O. Gayer, Z. Sacks, E. Galun, and A. Arie, "Temperature and wavelength dependent refractive index equations for MgO-doped congruent and stoichiometric $LiNbO_3$," Appl. Phys. B **91**, 343–348 (2008).

1. Introduction

Quasi-phase-matching (QPM) nonlinear devices, such as periodically poled lithium niobate (PPLN) and lithium tantalite (PPLT), have been widely studied in the field of nonlinear optical interactions because of their capability of achieving the desired phase-matching condition by spatially modulating the quadratic nonlinearities [1]. More important, possible engineering of QPM structures has afforded new degree of freedom in the nonlinear process. Recent attention has been given from uniform structure to Fibonacci optical superlattice [2], linearly chirped [3], apodized [4, 5], multi-segmented [6], and aperiodically QPM gratings [7, 8], which can provide more spatial reciprocal vectors to compensate for nonlinear phase mismatch in the broadband nonlinear process and multi-wavelength second harmonic generation (SHG). Engineered QPM structures also are used in controlling the cascaded quadratic nonlinearities in the phase mismatched SHG process by varying the local phase mismatch, which were used to achieve the tunable-chirp pulse compression [9], quadratic nonlinearity management [10] and two-color pulse compression based on quadratic nonlinearities [11]. Recently ultralow-power frequency-resolved optical gating (FROG) was demonstrated by using aperiodically poled lithium niobate (APPLN) because of adequate bandwidth for SHG in Ref. [12]. Thus the period qualities

#167192 - $15.00 USD Received 23 Apr 2012; revised 19 Jun 2012; accepted 21 Jun 2012; published 27 Jun 2012

of such non-uniform QPM gratings become crucial in the applications. Usually Hydrofluoric (HF) acid etching method is used to characterize the quality of domain-reversed structure but unavoidably destroy the crystal surface.

We show an approach to reconstruct quasi-phase-matching gratings by using a discrete layer-peeling (DLP) algorithm. DLP method was proven to be a simple, accurate and efficient approach to reconstruct the local structure of refractive index of fiber bragg grating [13–16] and other optical devices [17]. However, as far as we know, no work has been reported yet on the synthesis of QPM structure.

Chen et al. first demonstrated narrow-band Šolc-type wavelength filters experimentally based on PPLN crystal, which is sandwiched in the crossed polarizers [18]. By applying the external electric field along the transverse direction or using the misalignment of LN crystal orientation, the optical axes of ferroelectric domains are alternately rotated with the folded azimuth angle θ in successive reversal domains, thus PPLN is similar to so-called folded Šolc filter structure with periodically alternating azimuth angles of the crystal axes [19]. Polarization-independent [20] and narrowband multi-wavelength Šolc-type wavelength filters [21–23] in APPLN and bandwidth control by using local temperature gradient technique [24] were demonstrated in Šolc-type wavelength filters. By confining the light in the waveguides, efficient optical wavelength filter were recently reported [25, 26].

The ordinary and extraordinary waves propagating in QPM gratings are phase-matched due to the reciprocal vectors from the modulation of electro-optical (EO) coefficient in Šolc-type filters, which can be considered as a grating-assisted co-directional coupler, such as long period fiber grating based on refractive index modulation in the coupling region. Therefore the polarization coupling in QPM gratings can be described by using co-propagating coupling mode theory [27]. The grating-assisted co-directional coupler is usually treated as a finite-impulse-response (FIR) filter and each point in the impulse response is determined by the entire grating [28, 29]. We successfully use DLP algorithm to reconstruct the poling structure of QPM gratings in this work.

2. Numerical method and analysis

The coupling between ordinary and extraordinary waves in QPM gratings is described by the well-known coupled-mode equations as follows [19]:

$$\frac{dA_o(z,\Delta\beta)}{dz} = -i\kappa(z)A_e\exp(i\Delta\beta z) \tag{1a}$$

$$\frac{dA_e(z,\Delta\beta)}{dz} = -i\kappa^*(z)A_o\exp(-i\Delta\beta z) \tag{1b}$$

$A_o(z,\Delta\beta)$ and $A_e(z,\Delta\beta)$ represent the normalized amplitudes of ordinary and extraordinary waves, respectively, which can be considered as slowly varying amplitudes of co-directional propagating waves. $\kappa(z) = -\sin(2\theta)\frac{\omega}{c}\frac{n_e^2-n_o^2}{4\sqrt{n_o n_e}}e^{i\left[\frac{\pi}{2}+\phi(z)\right]}$ is the coupling coefficient along QPM grating [19], while $\phi(z) = [2\pi/\Lambda(z) - 2\pi/\Lambda_0]z$ denotes the local phase variation induced by QPM grating chirp in ununiformed QPM structures, and n_o and n_e are refractive indices of ordinary and extraordinary waves. The detuning parameter $\Delta\beta$ for QPM structure is defined as: $\Delta\beta = (\beta_o - \beta_e) - 2\pi m/\Lambda_0$, β_o and β_e are wave vectors of ordinary and extraordinary waves and $\Lambda_0 = \lambda_0/(n_o - n_e)$ represents the reference grating period and m is the ordinary QPM order. The polarization coupling between co-directional propagating waves occurs at the resonance frequency ω_0 when satifaying the phase matching condition: $\Delta\beta(\omega_0) = 0$. The local coupling coefficients are determined by the difference of refractive indices $\Delta n = n_o - n_e$ and QPM grating period $\Lambda(z)$ simultaneously. We assume the dispersion of refractive index negligible and keep

#167192 - $15.00 USD Received 23 Apr 2012; revised 19 Jun 2012; accepted 21 Jun 2012; published 27 Jun 2012

Δn constant in the simulation. Now that we need to figure out the period distribution of QPM gratings from the coupling coefficient $\kappa(z)$.

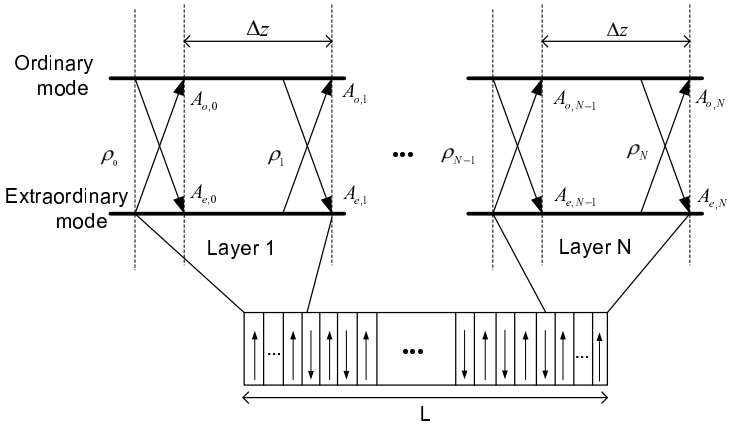

Fig. 1. The discretized coupling model of ordinary and extraordinary waves based on QPM structure.

The QPM structure is divided into N layers of uniform sections separated by a distance Δz. The discretized coupling model is illustrated in Fig. 1. Based on the piecewise uniform coupling model [30], we can separate the distributed coupling between ordinary and extraordinary waves into a stack of discrete instantaneous scattering points.

$$\begin{bmatrix} A_{o,j+1}(\Delta\beta) \\ A_{e,j+1}(\Delta\beta) \end{bmatrix} = G_\Delta G_\rho \begin{bmatrix} A_{o,j}(\Delta\beta) \\ A_{e,j}(\Delta\beta) \end{bmatrix} \tag{2}$$

where $G_\Delta = \begin{bmatrix} \exp(i\Delta\beta\Delta z) & 0 \\ 0 & \exp(-i\Delta\beta\Delta z) \end{bmatrix}$;$G_\rho = (1+|\rho|^2)^{-\frac{1}{2}} \begin{bmatrix} 1 & \rho \\ -\rho* & 1 \end{bmatrix}$.

The matrix G_Δ describes the pure propagation between the instantaneous scattering points and the other matrix G_ρ describes the coupling in the j-th layer of QPM structure [31]. ρ_j is the coupling strength of the instantaneous scattering point z_j along the structure. The discretized coupling coefficient $\kappa(z_j)$ can be obtained from the coupling strength ρ_j by using the following relation [27]:

$$\kappa(z_j) = -\frac{1}{\Delta z}\frac{\rho_j^*}{|\rho_j|}\arctan(|\rho_j|) \tag{3}$$

The main task now is to obtain the required strength ρ_j of the instantaneous scattering points from the transmission spectra. If the discretized coupling model is reformulated into the space-time domain, the discrete layer-peeling algorithm (DLP) by using the inverse-scattering method becomes efficient and is briefly introduced as follows (see details in Ref. [13, 16, 27, 31]). We define time delay with respect to the propagation of ordinary wave, i.e., ordinary wave propagates without time delay. The field vectors $a_{o(e),j}(\tau)$ in the time domain are related to the spectral fields by using a discrete-time Fourier transform [13, 16].

$$A_{o(e),j}(\Delta\beta) = \sum_{\tau=0}^{N} a_{o(e),j}(\tau)\exp(i2\Delta\beta\Delta z\tau) \tag{4}$$

where $\tau = 0, 1, \cdots, N$. The transfer matrix model defined in Eq. (2) can be transformed to time domain by replacing $A_{o(e),j}(z, \Delta\beta)$ with Eq. (4) [27]. We can obtain the time-domain response

#167192 - $15.00 USD Received 23 Apr 2012; revised 19 Jun 2012; accepted 21 Jun 2012; published 27 Jun 2012

in the j-th layer, which reveal the complex coupling strength ρ_j of QPM grating structure. The time-domain response is given as follows:

$$a_{o(e),j}(\tau) = \begin{bmatrix} a_{o(e),j}(0) & a_{o(e),j}(1) & \cdots a_{o(e),j}(N) \end{bmatrix} \tag{5}$$

It is known that the time domain field coefficients, $a_{o,j}(\tau)$ and $a_{e,j}(\tau)$ are discrete and correspond to the response of different time delay. $a_{o,j}(0)$ and $a_{e,j}(0)$ denote the two shortest time delay through QPM structure from causality requirements. At the end of QPM structure (layer N), the discrete coupling strength is simply expressed as:

$$\rho_N = \frac{a_{e,N}(0)}{a_{o,N}(0)} \tag{6}$$

Since the value of ρ_N is obtained from the output spectra, we can peel this layer off and calculate the impulse responses of layer $N-1$ by using transfer matrix method [27] and repeat the procedure until all the layers have been reconstructed. After the coupling strength is known, we can get the coupling coefficient $\kappa(z_j)$ of each layer from Eq. (3). The period chirp distribution of QPM grating can be obtained from the derivative of phase of the coupling coefficient by using Eq. (7).

$$\frac{d\phi(z_j)}{dz} = -\frac{2\pi z_j}{\Lambda_j^2}\frac{d\Lambda_j}{dz} \tag{7}$$

3. Experimental results and discussions

The setup of tunable Šolc-type filter based on QPM structure is shown in Fig. 2(a). A Z-cut MgO doped PPLN crystal is placed in the oven between two crossed polarizers and its temperature is precisely adjusted by using a temperature controller. The temperature instability is less than 0.1^{o}C. The PPLN crystal is fabricated by using electric-poling technique and the dimension is 50 mm (length), 12 mm (width) and 1 mm (thickness). There are one periodic QPM grating (3 mm width) with the nominal period 20.40 μm and two chirped gratings (3 mm width) with period change from 19.90 to 20.40 μm linearly and quadratically, respectively. We use a C + L broadband ASE source with an output wavelength range from approximately 1520 nm to 1610 nm and an optical spectrum analyzer (OSA) to detect the output light. The output spectrum of broadband ASE source used in the experiment is shown in Fig. 2(b). The following experimental transmission spectra of Šolc-type filter are normalized by the spectra of ASE source.

The typical measured transmission spectrum of Šolc-type filter based on uniform QPM grating is shown in Fig. 3(a) as the red dot line. It shows when temperature is 35.5 ^{o}C, the center wavelength is measured as 1589.44 nm, which is in good agreement with the theoretical prediction. The central wavelength of Šolc-type filter is tunable due to the temperature-dependent refractive indices [32] and wavelength tuning by changing the temperature is 0.60 nm/^{o}C.

We use the output spectra transmitted from the uniform and chirped QPM gratings to investigate the synthesis of different grating structures by using DLP algorithm. The uniform QPM grating is divided into $N = 200$ layers and the reconstructed period distribution by using DLP method is showed in Fig. 3(b). The result shows a good agreement with the theoretical expectation. The nominal chirped QPM gratings are expressed by $\Lambda(z) = \Lambda_0 + (\Lambda_N - \Lambda_0)(z/L)^m$, Λ_0, Λ_N is 19.90 μm and 20.40 μm, showing the linearly ($m = 1$) and quadratically ($m = 2$) chirped structures, respectively. Figures 4(a) and 4(b) show the measured transmission spectra of the linearly and quadratically chirped QPM gratings. We observe band-pass transmission spectra with some fluctuations in the middle wavelength region compared to the theoretical results.

#167192 - $15.00 USD Received 23 Apr 2012; revised 19 Jun 2012; accepted 21 Jun 2012; published 27 Jun 2012

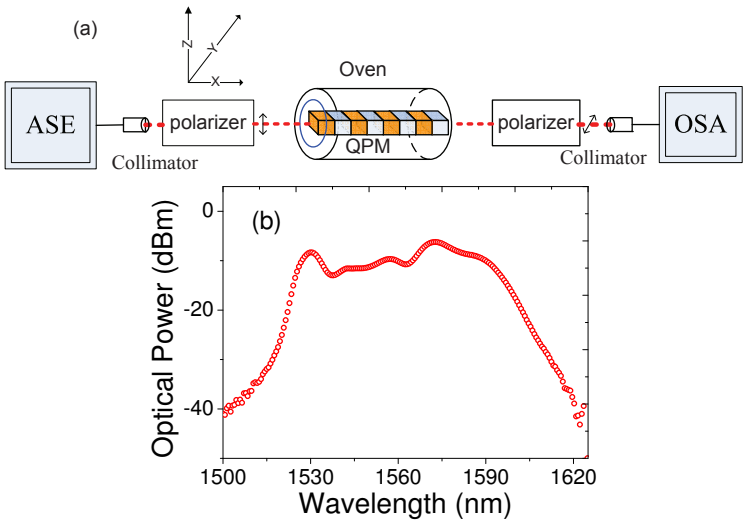

Fig. 2. (a) Experimental setup of tunable Šolc filter based on QPM structure; (b) the output spectrum of C+L broadband ASE source.

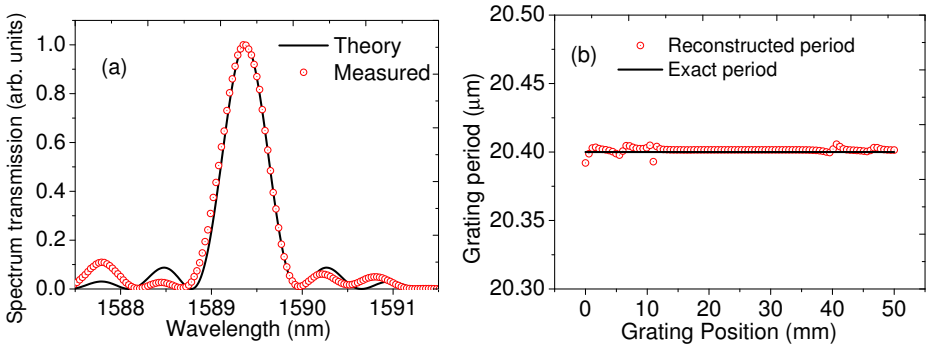

Fig. 3. (a) Normalized transmission spectrum at 35.5°C based on uniform QPM grating; (b) comparison between the reconstructed and the nominal uniform QPM gratings.

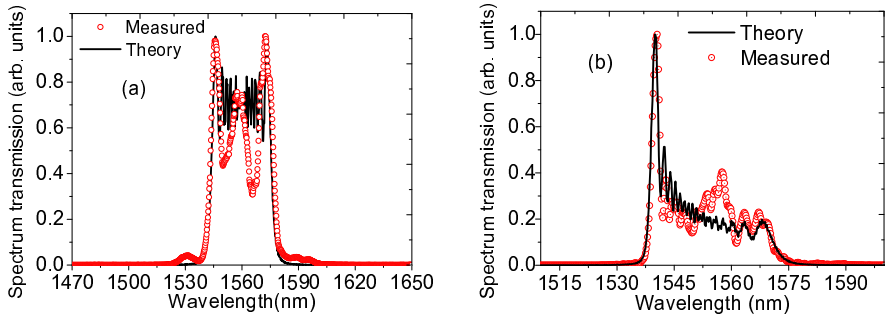

Fig. 4. Normalized transmission spectra (a) linearly chirped grating at 55°C; (b) quadratically chirped grating at 60°C.

#167192 - $15.00 USD Received 23 Apr 2012; revised 19 Jun 2012; accepted 21 Jun 2012; published 27 Jun 2012

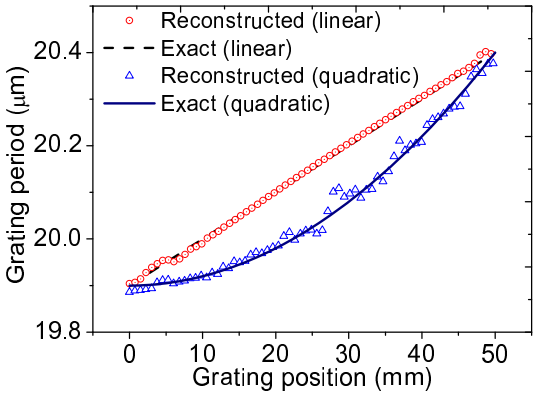

Fig. 5. Comparison between the reconstructed and nominal linearly and quadratically chirped QPM gratings.

The spectrum fluctuations are attributed to the possible deficiency of chirped QPM structures due to non-uniform electrical field distribution imprinted in QPM gratings during poling process. But the bandwidths of spectra are in good agreement with the theoretical results, which means that the grating periods at the input and output points are same with the nominal grating ones. We reconstruct the grating period distributions by using DLP algorithm and the results are shown in Fig. 5. The reconstructed linearly chirped QPM grating shows better agreement with pre-designed grating distribution than quadratically chirped grating, which indicates that manufacturing accuracy of local QPM period decrease when using the aperiodically grating pattern. The primary results show that it is possible to accurately inspect the period quality of QPM gratings without any etching destroys. We also admit that the output spectra are not fine enough and limit the accuracy of the synthesis on QPM grating.

4. Conclusion

We present an approach to retrieve the aperidically QPM grating structures efficiently and accurately by using the discrete layer-peeling algorithm. The measured output spectra of Šolc-type filter based on uniform and chirped QPM structures are used to reconstruct the grating structures, which show that the accuracy of local grating period decrease as the gratings become more complicated. This method has shown a potential application on the QPM grating design or the quality inspection during the fabrication.

Acknowledgments

This work was supported in part by the National Natural Science Foundation of China (60978004, 60937003, and 61132004), Shanghai Municipal Education Commission (10YZ14) and Shuguang Program (10SG38) and Shanghai Science and Technology Development Funds (11XD1402600), SSTCP (11511502501-2) and Leading Academic Discipline Project (S30108), and X.L. Zeng acknowledges the support of Marie Curie IIF(GA-2009-253289).

#167192 - $15.00 USD Received 23 Apr 2012; revised 19 Jun 2012; accepted 21 Jun 2012; published 27 Jun 2012